

Simulations of Foreground Effects for CMB Polarization

A. Kogut^{1,2} and G. Hinshaw¹

Accepted for publication in
The Astrophysical Journal

ABSTRACT

We use a simple model to investigate the effect of polarized Galactic foreground emission on the ability of planned CMB missions to detect and model CMB polarization. Emission from likely polarized sources (synchrotron and spinning dust) would dominate the polarization of the microwave sky at frequencies below 90 GHz if known Galactic foregrounds are at least 10% polarized at high latitude ($|b| > 30^\circ$). Maps of polarization at frequencies below 90 GHz will likely require correction for foreground emission to enable statistical analysis of the individual Stokes Q or U components. The temperature-polarization cross-correlation is less affected by foreground emission, even if the foreground polarization is highly correlated with the foreground intensity. Polarized foregrounds, even if uncorrected, do not dominate the uncertainty in the temperature-polarization cross-correlation for instrument noise levels typical of the MAP experiment. Methods which remove galactic signals at the cost of signal to noise ratio should carefully balance the value of rejecting faint foregrounds with the cost of increased instrument noise.

¹ Laboratory for Astronomy and Solar Physics, Code 685, NASA/GSFC, Greenbelt MD 20771.

² E-mail: Alan.Kogut.1@gsfc.nasa.gov.

1 Introduction

Polarization of the cosmic microwave background (CMB) provides a powerful probe of physical conditions and processes in the early universe. Following the detection of CMB temperature anisotropy, a great deal of theoretical effort has gone into calculating the polarized signal in various cosmological models (for a recent review, see Hu & White 1997). Precise maps of the polarization of the cosmic microwave background complement maps of the temperature anisotropy and offer the opportunity to break the parameter degeneracy that occurs in fitting temperature data alone (Zaldarriaga, Spergel, & Seljak, 1997; Efstathiou, & Bond, 1999; Kinney 1998).

CMB polarization is generated by Thomson scattering at recombination and is typically a small fraction of the temperature anisotropy. At expected amplitudes of only a few μK , polarized emission of cosmic origin could easily be masked by polarized foreground emission from the Galaxy. Little is known about the large-scale polarization of high-latitude Galactic emission. Synchrotron emission from electrons accelerated in the Galactic magnetic field is the dominant foreground at frequencies below ~ 20 GHz and is known to be linearly polarized. Extrapolation of radio polarization maps (Brouw & Spoelstra 1976) to millimeter wavelengths indicate a polarization fraction between 10% and 75% depending on Galactic latitude (Lubin & Smoot 1981). Free-free emission from electron-ion collisions in the interstellar medium was thought to be the brightest foreground at millimeter wavelengths, but remains largely un-mapped. Although free-free emission is expected to be unpolarized (except for small contributions from secondary Thomson scattering), recent work hints that additional microwave emission associated with infrared cirrus may have been mis-identified as free-free emission (Kogut et al. 1996, 1997; Leitch et al. 1997; de Oliveira-Costa et al. 1998, 1999). Radiation from spinning dust grains has been suggested as a possible mechanism for this anomalous emission (Ferrara & Dettmar 1994; Draine & Lazarian 1998, 1999). Thermal emission from vibrational modes in the grains should contribute negligibly to polarization at frequencies below 90 GHz, but electric dipole radiation from spinning dust is expected to be polarized as the dust grains align with the Galactic magnetic field, and could be a significant foreground at frequencies between 20 and 90 GHz.

Galactic emission is bright enough at microwave frequencies that even partial polarization could mask signals of cosmological interest. Several authors have investigated techniques to recover the cosmic signal in the presence of polarized foregrounds (Bouchet, Prunet, & Sethi 1999; Tegmark et al. 2000). These techniques use the average frequency and angular dependence of foreground emission to construct minimum-variance CMB maps subject to the constraint that emission matching these foreground dependences be cancelled. Although correct in principle, the foreground cancellation comes at a price in sensitivity. The linear combination of frequency channels designed to suppress foreground emission is weighted by the frequency

dependence of the cosmic and foreground signals and is significantly noisier than a simple noise-weighted sum. Bouchet et al. (1999) conclude that the forthcoming MAP mission, corrected in this fashion, will have only marginal sensitivity to CMB polarization in the presence of polarized foregrounds.

Foreground removal involves a tradeoff between instrument noise and foreground residuals; the optimum strategy depends on both quantities. Methods appropriate in the limit of bright contaminating foregrounds may not be necessary if the foregrounds are sufficiently faint. We analyze simulated maps on 0.2° angular scales including models of polarized Galactic emission to determine whether the polarized foregrounds require detailed models of the emission sources, or if the effect is weak enough that simpler, more sensitive remedies can be employed.

2 Polarized Galactic Model

Galactic polarization at millimeter wavelengths is not known in any detail. Known foregrounds, though, do not closely mimic the specific polarization pattern expected for the CMB signal, suggesting that a toy model capturing the approximate amplitude and pattern of foreground polarization is sufficient. For example, the cosmological temperature-polarization cross-correlation is characterized by a bulls-eye pattern surrounding hot and cold spots. Foreground polarization, on the other hand, reflects the orientation of the Galactic magnetic field projected on the plane of the sky. In order for foregrounds to produce a bulls-eye, the magnetic field would have to point radially outwards from a single point. Such a pattern is inconsistent with measurements of the Galactic magnetic field inferred from either synchrotron or scattered dust polarization (Brouw & Spoelstra 1976; Mathewson & Ford 1970). Our simulations thus use a simple toy model of polarized Galactic emission intended to capture the important features of astrophysically plausible polarization without assuming detailed knowledge of the interstellar medium at high latitudes.

We adopt the empirical “correlation” COBE-DMR model (Hinshaw et al. 1996 Table 1) for the unpolarized Galactic intensity (Stokes I component), scaling the Haslam 408 MHz survey (Haslam et al. 1981) to model synchrotron emission, and scaling the DIRBE $100\ \mu\text{m}$ survey for both the dust and free-free (or spinning dust) components. We assume that the polarized Galactic emission is proportional to the unpolarized intensity, and model the Stokes Q and U components as

$$\begin{aligned} Q &= f \cos(2\gamma) I \\ U &= f \sin(2\gamma) I, \end{aligned} \tag{1}$$

where $f(l, b)$ is the fractional polarization, assumed to vary across the sky, and $\gamma(l, b)$ is the polarization angle defined with respect to meridians connecting the Galactic poles. Although we do not expect this to be true in detail, it provides a simple way to

model polarized emission while retaining the non-Gaussian features typical of diffuse Galactic emission processes.

We wish to determine whether Galactic contamination of a simple noise-weighted CMB map produces a significant degradation compared to the instrument noise. A detailed approach would produce separate Q and U maps for each Galactic emission component in each frequency channel, and then co-add the channels weighted by the instrument noise. For simplicity, we instead evaluate the various Galactic emission components at a single fiducial frequency, and then scale this multi-component intensity map to produce maps of the foreground Q and U polarization. We adopt fiducial frequency 40 GHz (the lowest the three co-added MAP channels) with mean fractional polarization $\langle f \rangle = 0.1$. The RMS amplitude of the resulting foreground Q or U fluctuations is $3.2 \mu\text{K}$. The choice of fiducial frequency and mean polarization fraction reflects a conservative estimate of likely foreground contributions averaged over the MAP channels at 40, 60, and 90 GHz. A pessimistic model with 70% synchrotron polarization and 10% dust polarization would produce RMS fluctuations of $3.0 \mu\text{K}$ in the Stokes Q or U components after co-adding the individual channel maps. Both synchrotron and spinning dust polarization, when averaged over the high-latitude sky, are likely to have smaller fractional polarization than this pessimistic case. The toy model thus produces a simple, conservative estimate for the amplitude and spatial distribution of foreground polarization.

At high latitudes, the foreground polarization angle γ tends to follow the known radio loops, showing coherent structure on the angular scales $\theta < 20^\circ$ relevant to the CMB signal (Mathewson & Ford 1970; Brouw & Spoelstra 1976). We approximate this behavior in our toy model by generating simulated fields $\gamma(l, b)$ with different coherence angles θ_c . We first populate each pixel with random $[x, y]$ coordinates drawn independently from a uniform distribution. We normalize each $[x, y]$ pair to unit amplitude in each pixel, and then smooth the resulting maps with Gaussian full width at half maximum $\theta_c = [0, 2, 5, 10, 30]$ degrees, respectively. After smoothing, we generate a new normalization n for each coordinate pair and assign $\gamma = \arctan(y, x)$ in the usual fashion. Smoothing a vector field on the surface of a sphere produces topological defects where the angle γ becomes undefined (the normalization $n \rightarrow 0$). To prevent these topological “kinks” in the smoothed fields from dominating the small-scale distribution of the Q and U components, we use the smoothed normalization n to define a spatially-varying polarization amplitude,

$$f(l, b) = a n(l, b) \tag{2}$$

to force the polarized emission to zero at each defect. The scale factor a is chosen so that the mean polarization fraction $\langle f \rangle = 0.1$ averaged over the full sky, compatible with the polarization fraction expected from the dominant foregrounds (synchrotron or spinning dust) at frequencies below 100 GHz.

Since our analysis involves only rotationally-invariant quantities (Eq. 3), the result can not depend on the coordinate-dependent orientation of γ in any one region,

but only on the *change* in orientation across that region. We employ the coherence angle to assure that the orientation in our toy model remains nearly constant on scales $\theta < \theta_c$. By varying the value of θ_c we investigate the dependence of our results on the local coherence of the polarization angle, ranging from incoherent ($\theta_c = 0$) to coherent over large regions ($\theta_c = 30^\circ$).

3 Simulations

We use simulated maps of cosmic and Galactic emission to examine the effects of polarized Galactic foregrounds on the ability to detect a cosmic polarization signal. For clarity, we specialize to the parameters of the planned MAP mission (Bennett et al. 1995), although the results are applicable to a broad range of CMB missions. We use the CMBFAST power spectra (Seljak & Zaldarriaga 1996) smoothed with a 0.2° beam and generate random realizations of CMB sky maps in Stokes I, Q, and U components, including the proper correlation between the temperature and polarization. For the purposes of this paper, we restrict analysis to two input models: standard CDM and a reionized model (optical depth $\tau = 0.5$) with significant large-scale polarization. Both models have degree-scale polarization produced at the recombination epoch; reionization adds additional polarized emission on scales of tens of degrees. To each realization we then add Galactic emission (Eq. 1) and random realizations of instrument noise. The mean noise per $0.2^\circ \times 0.2^\circ$ pixel is $27 \mu\text{K}$ for Stokes I and $37 \mu\text{K}$ for Q or U, consistent with the noise properties of the co-added MAP data in the 40, 60, and 90 GHz channels over a 2-year mission. There is negligible correlation between the noise in the intensity and polarization maps.

Each realization of the sky includes random CMB and noise contributions, but uses nearly the same Galactic model. The only changes in the Galactic model result from changing the polarization templates $\gamma(l, b)$ in each realization by adding a constant γ_0 drawn from a uniform population $[-\pi, \pi]$. This effectively changes the mix of Q and U components in a given pixel from realization to realization, while retaining a fixed correlation between Galactic intensity and polarization amplitude. We repeat the simulations with different values of the coherence angle θ_c to investigate the effect of large-scale coherence in the foreground polarization angle γ .

We restrict analysis to the cut sky with latitude $|b| > 30^\circ$. For such partial sky coverage, the correlation function

$$C(\theta) = \frac{1}{N_{ij}} \sum_{ij} T'_i T'_j, \quad (3)$$

is a simple, powerful statistic for analyzing the sky signal, where the sum is restricted to pixel pairs $\{i, j\}$ separated by angle θ . The Stokes Q and U components depend on a specific choice of coordinate system and are not rotationally invariant. All sums

in Eq. 3 use rotationally-invariant quantities T' , defined as

$$\begin{aligned}
 Q' &= Q \cos(2\phi) + U \sin(2\phi) \\
 U' &= U \cos(2\phi) - Q \sin(2\phi) \\
 I' &= I,
 \end{aligned}
 \tag{4}$$

where the angle ϕ rotates the coordinate system at pixel i about the outward-directed normal vector to put the meridian along the great circle connecting pixels i and j (Zaldarriaga & Seljak 1997; Kamionkowski, Kosowsky, & Stebbins 1997).

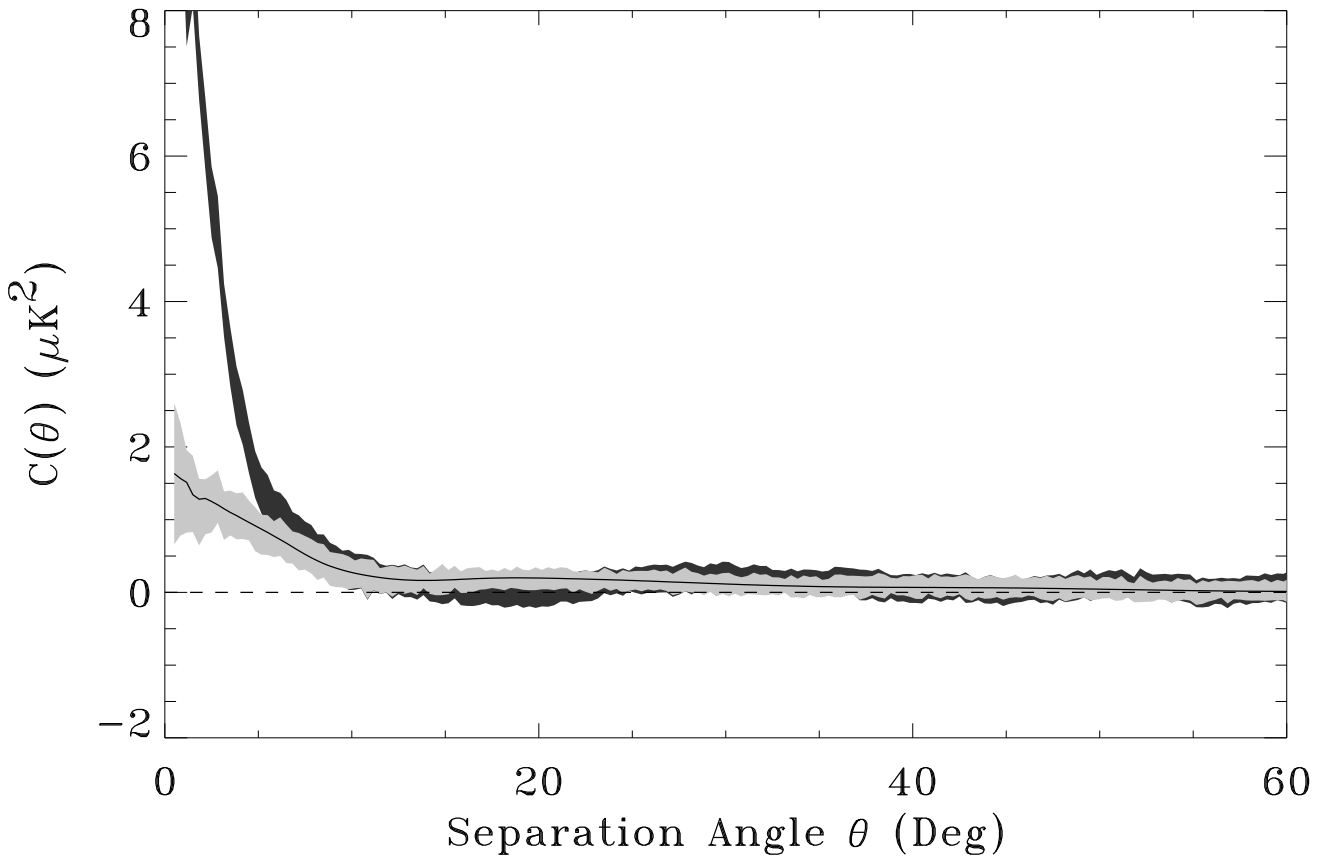


Figure 1: Auto-correlation function of polarized emission (Q component) for a reionized CDM model. The gray bands show the 68% confidence range in each angular bin for models with (dark band) and without (light band) foreground polarization. All models include Sinstrument noise scaled to the MAP 2-year mission. The solid line shows the CMB input used to generate the simulations. Polarized Galactic emission completely dominates the CMB and noise and biases the polarization autocorrelation, even for small fractional polarization $f \sim 0.1$.

4 Discussion

Figure 1 shows the QQ auto-correlation function for 100 realizations of a reionized CMB model with and without Galactic emission. The Galactic signal dominates the fainter cosmic signal, even for models with maximal CMB polarization. Direct detection of the cosmic Q or U polarization components using the individual Q or U polarization maps requires weaker Galactic polarization, higher observing frequency, and/or detailed modeling such that

$$\frac{Q}{3 \mu\text{K}} \left(\frac{\nu}{\nu_0} \right)^\beta \frac{\delta P}{P} < 0.3, \quad (5)$$

where ν_0 is the effective frequency of the co-added data, β is the spectral index of the foreground polarization, and $\delta P/P$ represents the fractional uncertainty in any galactic correction applied to the polarization maps.

The intensity-polarization cross-correlation provides a more robust probe of cosmic polarization. Galactic intensity is uncorrelated with CMB intensity. Even if the amplitude of polarized foregrounds is correlated with the unpolarized foreground intensity (Eq. 1), the dependence of the Stokes Q component on the polarization angle γ makes it equally likely to be positive or negative near individual foreground features. Figure 2 shows the mean cosmological signal for the IQ cross-correlation in the Λ CDM model. With no polarized foregrounds (light gray band), the cosmic signal at $\theta \approx 1.3^\circ$ is significant at 34 standard deviations for MAP 2-year noise levels. When polarized foregrounds are included (dark band), the significance falls to 31 standard deviations, still a highly significant detection: unmodeled Galactic foregrounds are unlikely to seriously degrade the IQ cross-correlation.

Polarized foregrounds do not bias the cross-correlation, but simply introduce an additional noise term. This additional noise term must be accounted for in any quantitative analysis. A commonly used statistic for model fitting is χ^2 , defined as

$$\chi^2 = \sum_{ab} \Delta C_a \mathbf{M}_{ab}^{-1} \Delta C_b, \quad (6)$$

where $\Delta C = C_{\text{obs}} - \langle C_{\text{model}} \rangle$ is the difference between the observed correlation function C_{obs} in any given realization and the mean $\langle C_{\text{model}} \rangle$ from some theoretical model, \mathbf{M} is the corresponding covariance matrix, and the subscripts a and b refer to angular bins. We investigate the effects of foregrounds by computing χ^2 for simulations with and without polarized signals, assuming either perfect knowledge or no knowledge of the foreground signal covariance. Table 1 shows the mean χ^2 (Eq. 6) for 100 realizations of the simulated IQ cross-correlation function for the Λ CDM model and $\theta_c = 5^\circ$ (the results do not depend strongly on the Galactic coherence angle). Each row shows the mean χ^2 of 100 realizations, analyzed using different assumptions for $\langle C_{\text{model}} \rangle$ and \mathbf{M}^{-1} (computed from the simulations), corresponding to models with

and without polarized emission. The different rows show the effect of changing the input data set while keeping model assumptions unchanged. Different columns show the effect of different model assumptions for a single data set.

Polarized Galactic emission does not prevent a significant detection of cosmological signal. If the input data contains cosmological polarization but unpolarized foregrounds (row PU), the increase in χ^2 when the model assumes no cosmic polarization allows us to reject this null hypothesis at 34 standard deviations (columns UU–PU). In the likely case that the sky contains significant unmodeled foreground polarization, we would calculate χ^2 using the same model functions as before (since we lack knowledge of the correct functions including foregrounds) but with input data now containing both cosmic and foreground polarization (row PP). Two effects are apparent: we still reject the null hypothesis, but the high χ^2/DOF indicates that the data are not well represented by the model.

The first two rows of Table 1 show that polarized foreground emission is unlikely to falsify a detection in the IQ cross-correlation if a cosmic signal exists. The third row demonstrates that polarized foregrounds are also unable to mimic

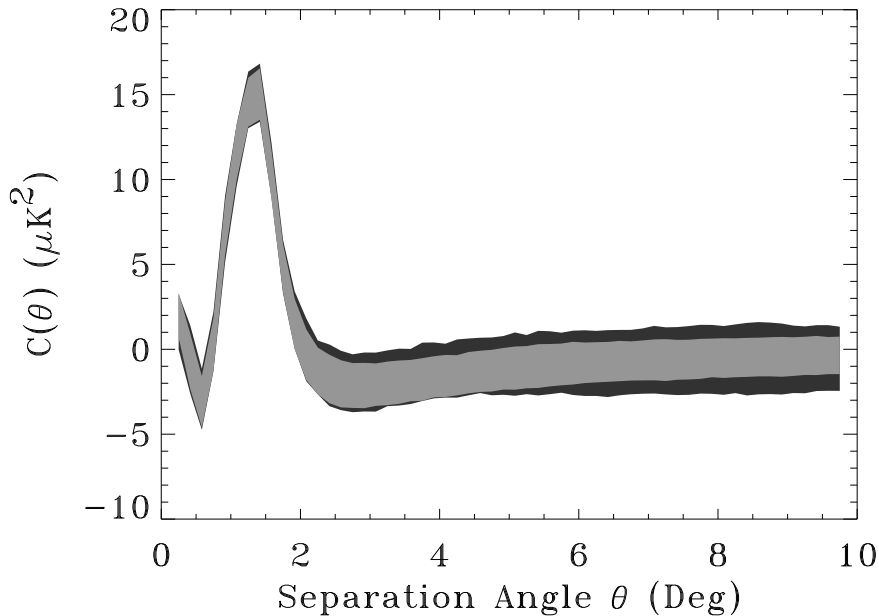


Figure 2: Temperature-polarization IQ cross-correlation for the Λ CDM model. The light grey band shows the 68% confidence range for 100 simulations of CMB and instrument noise. The outer (darker grey) band shows the 68% confidence range including polarized Galactic emission with coherence angle $\theta_c = 5^\circ$.

Table 1: Mean χ^2 for Simulated IQ Cross-Correlation

Data Polarization	Model Polarization			
	PP ^a	PU	UP	UU
PP ^a	59	92	397	499
PU	61	59	365	433
UP	473	568	59	111
UU	457	537	34	59

^a Letter pairs refer to polarized (P) or unpolarized (U) emission for the CMB and Galaxy, respectively: PU indicates polarized CMB emission and unpolarized Galactic emission, while UP indicates unpolarized CMB emission and polarized Galactic emission. Each χ^2 value uses 59 angular bins.

a cosmic signal in the event that the CMB is, in fact, unpolarized. Even if the only signal in the Q or U maps comes from foreground emission correlated with the foreground intensity, the shape of the resulting IQ cross-correlation function in any single realization is sufficiently different from the expected cosmic signal to reject a cosmic origin at high statistical confidence. As before, the poor χ^2 of the UP data fitted to the UU model indicates that additional unmodelled signals exist in the data; with such high signal to noise ratio, the correlation functions in the individual frequency channels could then be used to help identify the source.

A rotationally-invariant correlation function is simple to compute and is insensitive to details of noise coverage or the removal of pixels near the Galactic plane. However, predictions for CMB polarization are more commonly expressed in terms of the power spectrum, which is much more difficult to extract from partial sky maps. Since the power spectrum is the Legendre transform of the 2-point correlation function, we may approximate the cut-sky power spectrum by calculating the Legendre transform of the cut-sky correlation function for each realization, then averaging over realizations at each multipole ℓ . To speed the Monte Carlo simulations, we only compute each correlation function over the region $\theta < 10^\circ$ where the cosmological signal is largest. This truncation is equivalent to smoothing the power spectrum with a filter of full width at half maximum $\Delta\ell \approx 20$. Window effects from the Galactic cut are substantially smaller.

Figure 3 shows the IQ power spectrum from the same Λ CDM data as Figure 2, along with the theoretical power spectrum used to generate the polarized maps. The simple approximation is seen to be valid (up to minor “ringing” from the Galaxy cut)

and provides a quick representation of the data in a form readily comparable to theory. We use this approximation to quantify the relative contributions of instrument noise and foreground emission to the IQ cross-correlation. We define $R = \delta C'_\ell / \delta C_\ell$ as the ratio of the scatter at each multipole for models with foregrounds ($\delta C'_\ell$) compared to models without foregrounds (δC_ℓ), where both models include the cosmic signal and instrument noise. The ratio R is similar to the degradation factor DF of Tegmark et al. (2000), except for the foreground cleaning used therein. It differs from the “quality factor” of Bouchet et al. (1999), which compares the recovered signal C'_ℓ to the true (noiseless) sky signal. The ratio R shows the effect of the foregrounds *only* and thus separates the question of foreground removal (to correct or not to correct) from experiment design (choice of observing frequencies and noise level). The ratio R is plotted in the bottom panel of Figure 3 for several values of foreground coherence angle θ_c .

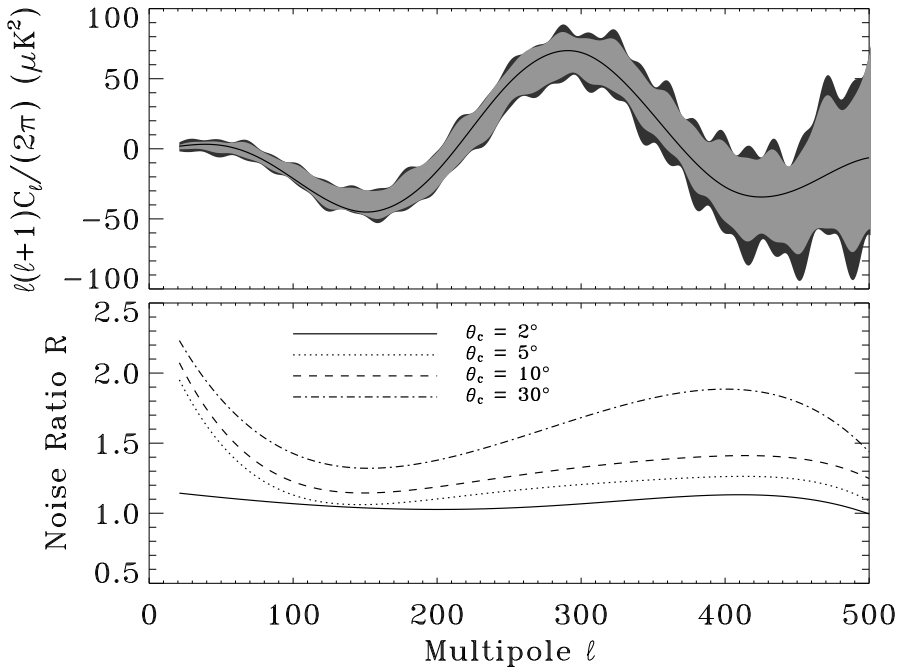


Figure 3: (top panel) Temperature-polarization power spectrum derived from the Legendre transform of individual correlation functions. The dark and light bands show the 68% confidence range for 100 simulations with and without polarized foregrounds, respectively. The solid line indicates the theoretical power spectrum used to generate the input correlation functions. (bottom panel) Ratio R of the scatter at each multipole for models with foregrounds compared to models without foregrounds. All simulations include CMB and instrument noise. Polarized foregrounds do not dominate the effective noise.

Since polarized foreground emission does not bias the mean cosmological signal, we can treat it as an additional noise term which adds in quadrature with the cosmic variance and instrument noise. By fitting the ratio R to models with different polarization amplitudes Q and correlation angles θ_c , we derive an approximate relation

$$R \approx \left[1 + 0.12 \left(\frac{Q}{3 \mu\text{K}} \right)^2 \left(\frac{\theta_c}{2^\circ} \right)^{0.9} \right]^{0.5} \quad (7)$$

for high-latitude data with MAP two-year noise and $\ell < 500$, where the foreground amplitude Q is evaluated at the effective frequency of the co-added CMB maps. Likely polarized foregrounds do not dominate the noise budget for the temperature-polarization cross-correlation; foreground removal techniques that increase the effective instrument noise by more than 30% are likely to do more harm than good.

5 Conclusions

We use simulations to investigate the effect of polarized Galactic foreground emission on the ability of planned CMB missions to detect and model CMB polarization. Emission from likely polarized sources (synchrotron and spinning dust) would dominate the polarization of the microwave sky at frequencies below 90 GHz if the high-latitude Galactic foregrounds are 10% polarized on average. Detection of a cosmic signal in the Stokes Q and U parameters would then require additional effort (using multi-frequency maps) to model and separate Galactic from cosmic emission.

Cross-correlation of the temperature and polarization maps provides a more robust method to detect CMB polarization, even if the foreground polarization is well correlated with the foreground intensity. Polarized foregrounds twice as bright as the CMB polarization still allow detection of the CMB signal at more than 31 standard deviations in the IQ cross-correlation for noise levels appropriate to the forthcoming MAP mission. The uncertainty in the recovered temperature-polarization power spectrum is dominated by cosmic variance and instrument noise, not by the additional “noise” caused by foregrounds. Methods that reduce the foreground signal using linear combinations of multi-frequency data can do more harm than good if the increase in instrument noise in the corrected data is larger than the foreground “noise” in the un-corrected data.

This work was supported in part by the Long Term Space Astrophysics research program under NASA RTOP 399-20-61-01.

References

- Bennett, C. L., et al. 1992, ApJL, 396, L7
Bennett, C. L., et al. 1995, BAAS, 187, 7109; <http://map.gsfc.nasa.gov/>
Bouchet, F. R., Prunet, S., and Sethi, S. K. 1999, MNRAS, 302, 663
Brouw, W. N., and Spoelstra, T. A. 1976, A&AS, 26, 129
de Oliveira-Costa, A., et al. 1998, ApJL, 509, L9
de Oliveira-Costa, A., et al. 1999, ApJL, 527, L9
Draine, B. T., and Lazarian, A. 1998, ApJL, 494, L19
Draine, B. T., and Lazarian, A. 1999, ApJL, 512, 740
Efstathiou, G., and Bond, J. R. 1999, MNRAS, 304, 75
Ferrara, A., & Dettmar, R.-J. 1994, ApJ, 427, 155
Haslam, C. G. T., et al. 1981, A&A, 100, 209
Hinshaw, G., et al. 1996, ApJL, 464, L25
Hu, W., and White, M. 1997, New Astron., 2, 323
Kamionkowski, M., Kosowsky, A., and Stebbins, A. 1997, PRD, 55, 7368
Kinney, W. H. 1998, PRD, 58, 123506
Kogut, A., et al. 1996, ApJL, 464, L5
Kogut, A. 1997, AJ, 114, 1127
Leitch, E. M. et al. 1997, ApJL, 486, L23
Lubin, P., and Smoot, G. 1981, ApJ, 245, 1
Mathewson, D. S., and Ford, V. L. 1970, Mem. R. Ast. Soc., 74, 139
Reach, W. T., Franz, B. A., Kelsall, T., & Weiland, J. L. 1995, *Unveiling the Cosmic Infrared Background*, ed. E. Dwek, (New York:AIP)
Seljak, U., and Zaldarriaga, M. 1996, ApJ, 469, 437
Tegmark, M., Eisenstein, D. J., Hu, W., and de Oliveira-Costa, A. 2000, ApJ, in press
(preprint astro-ph/9905257)
Zaldarriaga, M., Spergel, D., and Seljak, U. 1997, ApJ, 488, 1
Zaldarriaga, M., and Seljak, U. 1997, PRD, 55, 1830